ISSN 0915-633X

NATIONAL INSTITUTE FOR FUSION SCIENCE

Applications of Non-resonant RF Forces for Improvement of Tokamak Reactor Performances
Part I: Application of Ponderomotive Force.

T. Watari, R. Kumazawa, T. Mutoh, T. Seki, K. Nishimura
and F. Shimpo

(Received – Mar 19, 1993)

NIFS-220 May 1993

RESEARCH REPORT
NIFS Series

NAGOYA, JAPAN

Applications of Non-resonant RF Forces for Improvement of Tokamak Reactor Performances
Part I : Application of Ponderomotive Force.

T. Watari, R. Kumazawa, T. Mutoh, T. Seki, K. Nishimura, F. Shimpo

National Institute for Fusion Science
464-01, Chikusa-ku, Furo-cho, Nagoya , Japan

ABSTRACT

Applications of Radio Frequency to a tokamak diverter plasma for improvement of its reactor relevancy is studied and proposed. RF is applied to a diverter region of a tokamak by use of wave guide launchers on consideration of a reactor environment. Since the ponderomotive force is dependent on the charge to mass ratio of ions, various useful applications are considered. They covers some of the recent key issues in the developmental research toward nuclear fusion: the reduction of the heat load on the diverter plate, improvement of tritium inventory, impurity control, and helium ash removal.

KEY WORDS:

tritium saving, diverter heat load reduction, helium ash removal, impurity control, ponderomotive force, ITER, LHD

I. INTRODUCTION

A lot of achievements have been made in the area of application of RF to controlled thermonuclear fusion. Particularly, its application to plasma heating and current drive were so successful that they are envisaged as key components in the International Tokamak Engineering Reactor(ITER). Thanks to the design work done in the CDA(conceptual design activity), one can now conceive of a concept of ITER. EDA (Engineering Design Activity) began since 1992, where a more solid design is required based on the verification of the ideas via Research and Development (R&D) activities. Notwithstanding the recent progress shown in the big three tokamaks, it seems that there are some more problems to be solved before self-consistent design has been accomplished. They include: 1) reduction of heat load on the first wall, 2) alpha particle exhaust, 3)improvement of tritium inventory, 3) Impurity control, and 4) some new ways of current drive with high efficiency. In this paper, we try to give an assessment for applications of RF for such problems by use of non-resonant wave particle interactions. In section II, the forces acting on charged particles are classified into four parts. One of them is called ponderomotive force for which we will review a few integral results as base of the idea that we propose in this paper. In section III, A conceptual design of RF application which may withstand the reactor like environments is presented. In section IV, discussed are the possible contributions of such configuration by

clarifying related physics.

II. CLASSIFICATION OF THE FORCE ACTING ON PARTICLES.

In the discussion of this direction of research, we find it very convenient to use the formula proposed by Fukuyama and Itoh et al.[1]:

$$\begin{aligned}\vec{F} = \omega\varepsilon_0 (& \vec{k}/\omega \,\mathrm{Im}(\tilde{E}^* \cdot \chi_A \cdot \tilde{E}) \\ & -(\vec{k}/2\omega)\,\vec{\nabla}_r \cdot (\tilde{E}^* \cdot (\partial\chi_H/\partial\vec{k}) \cdot \tilde{E}) \\ & +(1/2\omega)\,\vec{\nabla}_r (\tilde{E}^* \cdot \chi_H \cdot \tilde{E}) \\ & -(1/\omega)\,\vec{\nabla}_r \cdot (\chi_H \cdot \tilde{E}\tilde{E}^*) \quad) \end{aligned} \qquad (1)$$

It has been known for long time that dissipative part of plasma response function to the applied rf is related to the wave particle interaction which accompanies energy and momentum transfer from wave to particles. The former has been used in plasma heating and the latter has been used in current drive. The first term in Eq.1 corresponds to this part of the effect of RF field on the plasma.

The second term which is proportional to $\vec{k}$ is related to wave refraction. The third therm, refered to as ponderomotive force,

has a form of gradient of a scaler potential. This term, vanishing when integrated over the plasma volume, does not yield any net force useful for current drive. However, it has been long used for suppression of the end loss of an open end confinement system[3].

The 4th term, which has a form of divergence of a tensor, was recently recognized as related to helicity injection. Since the applications of the dissipative part has been so intensively studied, we put more emphasis on the other three forces.

The 3rd term in Eq.1 is called ponderomotive force. With well known elements of the dielectric tensor given below,

$$\varepsilon_{XX} = 1 + \sum_j \chi^j_{XX}\,, \quad \varepsilon_{XY} = 1 + \sum_j \chi^j_{XY}\,, \quad \varepsilon_{ZZ} = 1 + \sum_j \chi^j_{ZZ}$$

$$\chi^j_{XX} = -\left(\frac{\omega^2_{p,j}}{\omega^2 - \omega^2_{c,j}}\right)\,, \quad \chi^j_{ZZ} = -\left(\frac{\omega^2_{p,j}}{\omega^2}\right) \qquad (2)$$

the well known formula of ponderomotive force is reproduced:

$$\vec{F}_j = -\vec{\nabla}\left(\frac{n_j q_j^2}{2 m_j}\left(\frac{\left|E^2_{\perp}\right|}{\omega^2 - \omega^2_{c,j}} + \frac{\omega^2_{p,j}}{\omega^2}\cdot\left|E^2_{//}\right|\right)\right) \qquad (3)$$

Since the first term dominates when RF frequency is chosen close to the cyclotron frequency, we will ignore the second term in the following arguments for simplicity. As obviously seen in

Eq.3, the gradient of wave field creates a force that expels particles if $\omega > \omega_{c,j}$. On the contrary, particles are attracted when $\omega < \omega_{c,j}$. If the electric field has gradient along the magnetic field, this force can be used for end plugging of an open-ended devise. This was the concept that guided RFC-XX project[3].

Figure 1 shows an experimental setup used in the principle proof of this idea . RF was applied by use of a pair of parallel plate electrodes. The end loss flux was measured by so called Faraday cups, or, in order to separate the species, time of flight type analyzer was used alternatively.

In Fig.2, shown is the experimental data demonstrating the reduction of the end loss of respective species. It is clearly shown that the degree of reduction is dependent on the applied frequency. End loss of each species is preferentially reduced with the corresponding ion cyclotron frequency. This is qualitatively consistent with the prediction of Eq. 3. With more close look at Fig.2, one may find the difference of the experimentally obtained optimum frequencies from their correspondent cyclotron frequency. This is explained in terms of the collective response of the plasma to the RF field[4]. However,this is not the subject of this paper and will not be discussed in this article in any more detail.

As the applied RF field is changed, the loss flux, α, decreases. As shown in Fig.3, the dependence of α on RF field intensity may be cast into a form of $\alpha = \exp(-c \cdot E^2)$ with c, a constant.

As an application of the force parallel to the magnetic field line, We may refer to the work by Ohkawa[5]. Here, ponderomotive force on electrons is applied in the diverter region, aiming at a formation of thermal barrier in order to facilitate an easier access to H-mode. Our proposal here contrasts to theirs by that we use the force acting on ions taking advantage of being mass and charge dependent.

Equation 1. predicts that there is force proportional to $\tilde{\nabla}_{\perp}|E_{\perp}|^2$ besides the force parallel to $\tilde{\nabla}_{//}|E_{\perp}|^2$. The application of this force has been examined theoretically and experimentally by several authors: Yasaka et al [6] proposed to use this force for the stabilization of interchange mode in a Mirror confinement system by compensating the bad curvature and demonstrated in a experiment. Successively, application of this force to stabilization of tokamak plasma against ballooning mode has been proposed by D'Ippolito et al.[7]. These theory and experiments dealt with the force acting on ions but, if we trace back history, we find also the work done by Magda et al.[8] which dealt with the force acting on the electrons.

III. A WAY OF APPLICATIONS OF RF TO IMPROVE REACTOR PERFORMANCE.

Here, in this paper, we propose to use ponderomotive force in the diverter region of a tokamak reactor. Let us imagine a set up shown in Fig.4. To make the circumstance clear, it has ITER

like magnetic configuration with either single null or double null diverters, it has large space outside the plasma core from the engineering requirement of having a blanket. We suppose that the plasma discharge is in a L-mode with comparatively low edge electron and ion temperatures.

In the bottom of the Fig.4, drawn are two wave guides which are introduced to apply the RF field in order to create the ponderomotive force. Drawn also are pumping ducts; recently a pumped diverter is assumed as a key function in reactor designs. Fig.5 gives an idea about how this proposal looks like 3-dimensionally. The number of wave guide is typically $N_0/2$ with N_0 the number of toroidal coils. The same number of pumping ducts are envisaged next to each other.

a) Electrostatic excitation of the wave (n=0 mode)

We are considering the case in which RF is applied perpendicularly to the magnetic field. There may be several ways in application of rf field. The one shown in Fig.5 is specified as n=0 mode with, n, the toroidal mode number. The toroidal trough structure shown in Fig.5 is a kind of resonator. The horizontal extension ℓ_1 is around a quarter of the free space wave length and the height ℓ_2 is optimize in the following consideration: for n=0 mode there is no RF magnetic field leaking out of the resonator. Only the RF electric field leaks out to the diverter leg plasma. This fringe effect is stronger with larger value of ℓ_2. Therefor a large ℓ_2 is favorable in

order to obtain large ponderomotive force. On the other hand the impedance of the resonator is lower with smaller ℓ_2 , which is favored from the technical point of view.

It is noted that the field lines at the null point direct toroidal direction. Figure 6(a) shows the way they whirl out from the null point along the diverter leg. Here, poloidal component of the static magnetic field is exaggerated for illustration; magnetic field lines of force do not deviate much from the toroidal direction. Since the rf field is in the poloidal direction , we are setting a situation to use the first term in Eq.3.

b) Magnetic excitation of the wave.

The application of RF via magnetic field has been proven its better quality compared to electro-static one in many ICRF heating experiments. The better performances of magnetic coupling have also been shown in the application of RF to open-end confinement system[9]. However, as we noticed in the previous subsection, we cannot obtain magnetic field extend out to the plasma as long as we work with n=0 mode. Therefore, we set the structure shown in Fig.7 and analyze the consequences. The toroidal trough is separated in 2N sections, each extending for $\phi_0 = \pi / N$ in toroidal angle. Then TE-mode is excited in each separated troughs with $\lambda_\phi = 2 \cdot \phi_0 \cdot R$ along the toroidal extension. The electric field is mostly perpendicular to the magnetic field and magnetic field can now leak out to the

plasma. The height of the resonator, ℓ_2, will be determined in the similar way as subsection (a). The depth of it, ℓ_1, is now given by

$$\ell_2 = 1/4 \cdot \left((1/\lambda_0)^2 - (1/\lambda_\phi)^2 \right)^{-1/2} \qquad (4)$$

where, λ_0 is the wave length in the free space. If there is not enough room to implement ℓ_1 given by Eq.4, a folded structure shown in Fig.8 will be used. The phase between the adjacent resonators can basically be either in-phase, opposite-phase, or dephased by changing frequencies relatively. Different from the ordinary case of plasma heating or current drive, the plan here does not need to heat particles. We need to minimize the wave absorption by particles, specifically by ions, in order to reduce the circulating power and impurity generation. This kind of idea, referred to as adiabaticity condition, was clarified several years ago in the context of RF Plugging of an open end loss[10]. Avoiding rigorous argument, this condition is given by

$$\omega - \omega_{c,i} \equiv \delta\omega \geq (\partial E/\partial \ell)/E \cdot v_{T,i} \ . \qquad (5)$$

reverse of which is well known as matching condition in the field of plasma heating and current drive. Here, ℓ is the length along the magnetic field line. The hight of the ponderomotive potential is expressed by

$$\Phi = \frac{n_j q_j^2 |E_\perp^2|}{2 m_j \omega^2} \cdot \frac{1}{2\delta} \qquad (6)$$

in terms of the δ defined in Eq.5. Therefore, $1/(2\delta)$ is regarded as a potential enhancement factor. We need to take δ as small as possible without violating the inequality(5).

With the instrumental set up shown in Fig.7, the potential contours and magnetic field lines intersects in the way shown in Fig.6(b). As it is clear in the comparison between Fig.6(a) and Fig.6(b), the scale length of RF field for n=0 and n=N cases are given respectively by

$$L^{-1} = (\vec{B} \cdot \vec{\nabla} E^2 / (B / E^2)) = (B_p / B) \cdot (1/E^2) \ (\partial E^2 / \partial \ell_p) \qquad (7)$$

and

$$L^{-1} = (\vec{B} \cdot \vec{\nabla} E^2 / (B / E^2)) = N \cdot (\pi R)^{-1} + (B_p / B) \cdot (1/E^2) \ (\partial E^2 / \partial \ell_p) \qquad (8)$$

Here, Bp, the poloidal magnetic field, is small near the null point making the first term of Eq.8 dominant. Therefore, we obtain from Eq. 5

$$\delta > v_{T,j} / (R \phi_0 \omega) \qquad (9)$$

Here, $R\phi_0 = R(\pi / N)$ is the toroidal extension of the resonator which should be reasonably large in order to minimize δ. It contrast to the analysis by Ohkawa [5] that a locally applied ponderomotive potential works well because the magnetic field points essentially the toroidal direction. It should be mentioned that ponderomotive force on electrons is treated in that paper where the inequality 9 is satisfied more easily due to its $\sqrt{m_e}$ dependence.

IV. VARIOUS POSSIBLE EFFECTS OF PONDEROMOTIVE FORCE

(1) Reduction of the heat load

One of the problems to be solved in successfully launching a reactor grade devices is the reduction of the heat load on the diverter plate. Though there may be some efforts to increase radiation loss from the edge of the main body of the plasma, some fraction of the total heat load will be conveyed by particles to diverter plate. Since this heat load is estimated to be so high that any existing material cannot endure, the remaining things to do is to disperse the width of the diverter leg so that heat deposition per unit area on the diverter plate is small. In the estimation of the diverter heat load, diffusion of the particles across the magnetic lines of force as they travels along the magnetic field. Here, it is customary that Bohm type anomalous diffusivity is used in diverter modelings,

which certainly assumes the presence of turbulence caused by some types of plasma instability. We propose to apply the ponderomotive force in order to increase the bad curvature. The plasma in the diverter leg has a sharp density gradient on both side of the separatrix. When pondero-motive force is applied, one of the sides satisfying

$$\vec{F}_j \cdot \vec{\nabla} p = -\vec{\nabla} p \cdot \vec{\nabla} \left(\frac{n_j q_j^2}{2 m_j} \left(\frac{|E_\perp^2|}{\omega^2 - \omega_{c,j}^2} \right) \right) < 0 \qquad (10)$$

will be subject to interchange type instability and increase the diffusivity. Subsequently, the thickness of the diverter leg is increased and dispersion of the heat flux at the first wall is attained relaxing the requirement imposed on the material. Though we may pay attention to any of the ion species specified by the subscript j in Eq.10, let us imagine deuterium for example with a frequency a little higher than deuterium cyclotron frequency. Under this circumstance, this scenario is compatible with the different use of the ponderomotive force shown in subsection (2) and (3). Finally, we note that the effect of the ponderomotive force on the plasma stability was demonstrated in several experiments as mentioned in the introduction: Yasaka et al [6] and Magda et al.[8]. The former used the force acting on ions and the latter used the force on electrons. Figure 9 shows existing data base showing such effect[3]. Here, an experimental setup as shown in Fig.1 is used and the spacial spread across the sheet plasma was measured. It is clearly demonstrated that the maximum heat load is reduced by

a factor larger than 10.

As an alternative set up, one can apply the RF from both side of the diverter plasma. Then, electric field E may take a parabolic profile across the diverter plasma giving $\vec{\nabla} p \cdot \vec{\nabla} E^2$ negative definite value across the diverter plasma. In such an experimental set up, the frequency must be chosen close but slightly lower frequency than the cyclotron frequency of chosen ion species.

(2) The application of ponderomotive force to improvement of tritium inventory.

Since there is no plentiful tritium resources in the world and due to its harmfulness to human bodies, economy of tritium is listed as one of the important issues in nuclear fusion [12]. We can take advantage of the fact that the ponderomotive force on ions is dependent on the charge to mass ratio in the application to this problem. Fig.10 show the case where a frequency slightly higher than tritium cyclotron frequency is applied. In this case, the potential is positive for tritium and negative for deuterium. The tritium ions with energy lower than the potential barrier is reflected back to the main body of the plasma causing a reduction of tritium particle flow by a factor of

$$R_T = \exp (-\phi_T / T_T) \qquad (11)$$

This minimizes the waste tritium feed to

$$\dot{N}_T - \dot{N}_{T,burn} = N_T \cdot R_T / \tau_{p,T} \qquad (12)$$

As an example we consider following parameters:
$T_T = T_D = T_e = 200\,eV$, $T_{He} = 600\,eV$, and $B_T = 5\,T$, If we choose $\omega = 1.1\,\omega_{c,T}$ and E=3kV/cm, the peak value of the potentials, Φ_T, Φ_D, and Φ_{He} are estimated to be 270V, -70V and -170V, respectively . Typically, RF field of E=5kV/cm, should creates the potential barrier of 750ev reducing the tritium loss flux by factor of 1/40.

(3) The application of ponderomotive force to helium ash removal.

The scenario shown above provides a effective way of tritium saving, by which He ash is exhausted relatively to tritium. It is possible as well to apply two frequencies: ω_1 slightly higher than tritium cyclotron frequency and ω_2 slightly higher than deuterium cyclotron frequency . Deuterium inventory, as well as tritium inventory, is improved in this case. However, because there are no difference in the Z/M ratio between deuterium and He ions, Eq.(3) indicates that the ponderomotive force is positive to He ions. Therefore, the application of

second frequency in not always beneficial from He ash removal point of view.

However, it is quite probable that peripheral He temperature is higher than other fuel ions. The edge Helium temperature is determined in the process that Alpha particles born at the center of the plasma, reduces energy in the collisions with electrons, and diffuses out toward plasma periphery. The peripheral ion temperature of fuel ions are determined in the process that it gets energy mostly from electrons at the core region and lose it in heat diffusion. If there is a difference between helium ion temperature and fuel ion temperatures, there is the difference in the recycling rates whose ratio is given by

$$\eta_{He,D} = R_{He} / R_D = \exp(-\phi_{He} / T_{He} + \phi_D / T_D) \qquad (13)$$

$$\eta_{He,T} = R_{He} / R_T = \exp(-\phi_{He} / T_{He} + \phi_T / T_T) \qquad (14)$$

With parameters $\omega_1 = 1.1\,\omega_{c,T}$, $\omega_2 = 1.1\,\omega_{c,D}$, $E_1 = 3\,kV/cm$, and $E_2 = 4\,kV/cm$, the potentials, ϕ_T, ϕ_D, and ϕ_{He} are calculated to be 320V, 230V, and 460 V, respectively, as shown in Fig. 11. This yields a modest values of the figure of merits: η(He,D)= 1.618 and η(He, T)=2.54. However, if edge He temperatures is around 1keV, they are enhanced to η(He,D)=3.3 and η(He, T)=6.6 with $E_1 = 3.9/cm$, and $E_2 = 5.2\,kV/cm$. Thus, the degree of improvement depends on the difference of the He ion temperature and those of fuels. As the degradation of global ion particle

confinement at high density is reported from many tokamaks. Such critical density is reached with smaller amount of fuel gas puffing with the ponderomotive barrier using two frequencies. The global confinement of the core plasma(including He ash) will then be degraded in proportion to the amount of gas puffing.

Throughout this paper, the model was simplified as much as possible. The role of the space potential, however, should be briefly mentioned. The reduction of the end loss will raise the space potential of the plasma relative to the wall potential in order to balance the electron and fuel end losses. It is known that the potential created in such a manner is given by

$$\phi_s = (Z_e / T_e + Z_{fuel} / T_{fuel})^{-1} \cdot \phi_{fuel} / T_{fuel} \qquad (15)$$

as He ash and impurity ions are treated as trace amount. This reduces the potential barrier of the He ash to

$$R_{He} = \exp ((- \phi_{He} + Z_{He} \cdot \phi_s) / T_{He}). \qquad (16)$$

When the effect of space potential is correctly taken into consideration, the recycling reduction rate expressed by Eqs. 13-14 is improved by a factor of

$$G_s = \exp (- (Z_{He} / T_{He} - Z_{fuel} / T_{fuel}) \cdot \phi_s) \qquad (17)$$

Due to the difference of Z between He and fuel ions, Eq.17

suggests that the space potential aids in pumping out He ash. Thus, inclusion of the space potential facilitates the idea of He ash removal even in the case of absence of temperature difference.

4) Impurity control

The same experimental set up as introduced in the previous subsections are useful also for impurity control which is one of the key issues in a tokamak reactor design.

In order for ponderomotive potential to be used for impurity control, potentials for impurity ions must be negative or sufficiently small while keeping those for fuel ions high.

The effectiveness of this scheme may vary according to the assumed electron temperature and also may be dependent on the chosen frequency. In order to avoid too many variations , we assume the same experimental set up as the previous section and describe the contribution of the ponderomotive force.

Two frequencies $\omega_1 = 1.1\,\omega_{c,T}$ and $\omega_2 = 1.1\,\omega_{c,D}$ as described in the previous section are used. The impurity ion temperature as well as electron temperature is assumed to be same as those of fuel ions, i.e., ~200eV.

Attention is paid to the fact that the degree of ionization proceeds as electron temperature increases and with Te~ 200ev impurity ions are populated over the various ionization stages with $\tilde{Z}_I / M_I$ ranging mostly from 1/2 to 1/3. The ions with $\tilde{Z}_I / M_I$ close to 1/2 feels the positive potential caused by the

RF field with frequency $\omega_2 = 1.1\,\omega_{c,D}$; this effect is rather harmful. However, as $\tilde{Z}_I / M_I$ decreases from 1/2, the negative ponderomotive potential due to the RF field with frequency $\omega_1 = 1.1\,\omega_T$ increases rapidly to cancel out the positive potential. The complete cancellation occurs at

$$\tilde{Z}_I = \sqrt{13/18}\,(M_I/M_D)\,Z_D\,(\omega_1/\omega_{c,D}) \approx 0.9\,Z_I \qquad (18)$$

That means most impurity particles feels negative potentials so that impurity ions are pumped out effectively. Inclusion of space potential into consideration yields the recycling rate,

$$R_I = \exp\left((-\phi_I + \tilde{Z}_I \cdot \phi_s)/T_I\right) \qquad (19)$$

from the similar calculation as Eq.16. The effect of space potential is much larger for impurity confinement than for other species, because $\tilde{Z}_I$ is larger compared to those of others. Therefore, the application of ponderomotive potential to impurity control is also promissing.

V. DISCUSSIONS

In specifying the hardware in section III, particular attention has been made to the fact that such equipment is durable against

the given neutron environment in a reactor use. Particularly, the use of week component like ceramic feed through was avoided. The size of the feeder wave guide may not be large enough to transmit the RF in VHF band. However, recent progress in ridged wave guide[14] and folded wave guide[15] almost get this concern away. Though this paper does not specifies coupling structure between the feeder to the resonator, there should be many good ideas because the cavity-Q of the resonator is expected to be large. The wave-particle interaction via ponderomotive force is essentially energy conserving and no power input to particles are predicted. Since the plasma at the diverter is so thin that all the fast waves are evanescent. Therefore, there is no wave to propagate out to the main plasma. The circulating power is then estimated by the loss in the resonator. This power is estimated to be a few MW, which does not increase circulating power in a significant level as this concept is applied to a reactor. Throughout this paper, we ignored collective response of a plasma. However it has been shown in the past experiment that ponderomotive potential can affect a plasma at a high density regime around 10^{13} ~10^{14} cm^{-3} with ion temperature of 10 eV [9] and at a temperature 100 ev and density around 10^{12} cm^{-3} [16]. The parameter range of such experiments are not necessarily far from our goal. An experiment in a medium size tokamak is needed in order for this idea to be used in ITER or reactor like tokamak. We specified the way of RF application to a wave guide resonator type only from a technological reason. It does not totally deny possibility of using conventional antennas. Use of it is rather recommended in a proof of

principle experiments. This paper treated the possibility of improving the tokamak performance by controlling the edge of the plasma. The possibility of applying various forces involved in Eq.1 to a problems of controlling the plasma at the core will be published elsewhere.

ACKNOWLEDGEMENTS

The author is grateful to Drs. K. Itoh, S.I. Itoh in National Institute for Fusion Science, and Dr. A. Fukuyama in Okayama University for clarifying discussions of Physics. The authors also would like to acknowledge the discussion with Y. Yasaka in Kyoto University and Dr. T. Shoji in Nagoya university. This work was possible on the basis of the RFC-XX project. We thanks Drs. T. Sato, T. Watanabe, and T. Hatori for the useful discussions. This work is also applicable to LHD projected undergoing at NIFS and partly motivated by it. The authers also thanks to Drs. T. Kuroda, M. Fujiwara, and A. Iiyoshi for continuous encouragement.

REFERENCES

[1] Fukuyama,A., Itoh,S.-I., Itoh,K., et al, Journal of Phys.Soc.Japan, 51(1982)1010

[2] Fukuyama,A., Itoh,S.-I., Itoh,K., et al, proc.13th IAEA Conf.on Plasma Physics and Cont.Nucl.Fusion Research, Washinton, 1990, IAEA, vol.1,p-855

[3] Sato,T., Takayama,K., "End Plugging and Cusp", IPPJ-REV-5, Institute of Plasma Physics,1989

[4] T. Watari, S. Hiroe, T. Shoji, et al., Phys. Fluids, 17(1974)2107,

[5] Ohkawa,T., "Kakuyugo Kenkyu",64(1990)305

[6] Yasaka,Y., Itatani, R., Nuclear Fusion 24(1984)445

[7] D'ippolito and J.R. Myra, Phys., Fluids 29(1986)2594

[8] Ericson, Magda, Ward, Seabury C., Brown, Sanborn C., Journal of Applied Physics, 33(1962)2429

[9] WATARI,T., HATORI, T., KUMAZAWA,R., et al., Phys. Fluids, 21(1978)2076

[10] Hatori, T., Watanabe, T., Nuclear Fusion, 15(1975)143

[11] Shoji,T., Grossman, A., Conn,R., et al., Journal of Nuclear Materials, 176$177(1990)830-836

[12] JET Team, Nuclear Fusion, 32(1992)187

[13] Greenwald. M., Gwinn, D., Milora.,et al., Physical Rev., Lett., 352(1984)352

[14] Arai,H., Goto, N., IEEE Transaction on Plasma Science , vol.PS-13, (1985)582

[15] Owens, T.L., IEEE Transactions on Plasma Science, vol.PS-14, (1986)934

[16] Kumazawa, R., Adati, K., Aoki, T., et al., J. Phys.Soc.Jpn., 57(1988)919

FIGURE CAPTIONS

Fig.1 The experimental set up used in the demonstration of end plugging using ponderomotive force. The RF was applied

electro statically by use of a parallel plate electrodes.

Fig.2 The reduction of the end loss of respective ion species. The end loss was measured by a time of flight type ion analyzer.

Fig.3 The reduction of end loss as the electric field was increased. The end loss was measured by use of a multi-grid type electro-static analyzer.

Fig.4 The concept of application of ponderomotive force to a diverter plasma of an ITER like large tokamak.

Fig.5 The artists view of a wave guide feeder and a resonator to apply RF field.

Fig.6 The magnetic lines of force in front of the resonator(solid lines) and the contour of the ponderomotive potential(broken lines); (a) the electro-static coupling case(the toroidal mode number, n=0) and the magnetic coupling case (the toroidal mode number, n=N).

Fig.7 The structure of the resonator and the feeder in the magnetic coupling case; the resonator trough is separated into 2N sections. The RF is fed by use of ridged wave guides or folded wave guides by which ceramic insulator is put away from the reactor core region.

Fig.8 The structure of the resonator: (a); high impedance coupling and (b); low impedance coupling. The resonator is like a wave guide folded in the direction of propagation so that the effective length comparable to

the $\lambda_0/4$ is obtained. The mouth of the resonator shown in (b) is partly short circuited. It resembles to a current strap antenna suggesting that use of antennas for the present purpose is possible as well.

Fig.9 Experimentally observed spreading of the diverter like sheet plasma as ponderomotive force is applied via parallel plate electrodes like in Fig.1.

Fig.10 The ponderomotive potentials applied for the purpose of tritium saving.
Following parameters are used in the calculation:
$\omega_{c,D} > \omega > \omega_{c,T}$, $\omega/\omega_{c,T} = 1.1$, $B_T = 5\,T$, and E=3kV/cm.

Fig.11 The ponderomotive potential applied for the purpose of He-ash removal. Following parameters are used in the calculation: $\omega_2 > \omega_{c,D} > \omega_1 > \omega_{c,T}$, $\omega/\omega_{c,T} = 1.1$, $B_T = 5\,T$, $E_1 = 3\,kV/cm$, and $E_2 = 4\,kV/cm$.

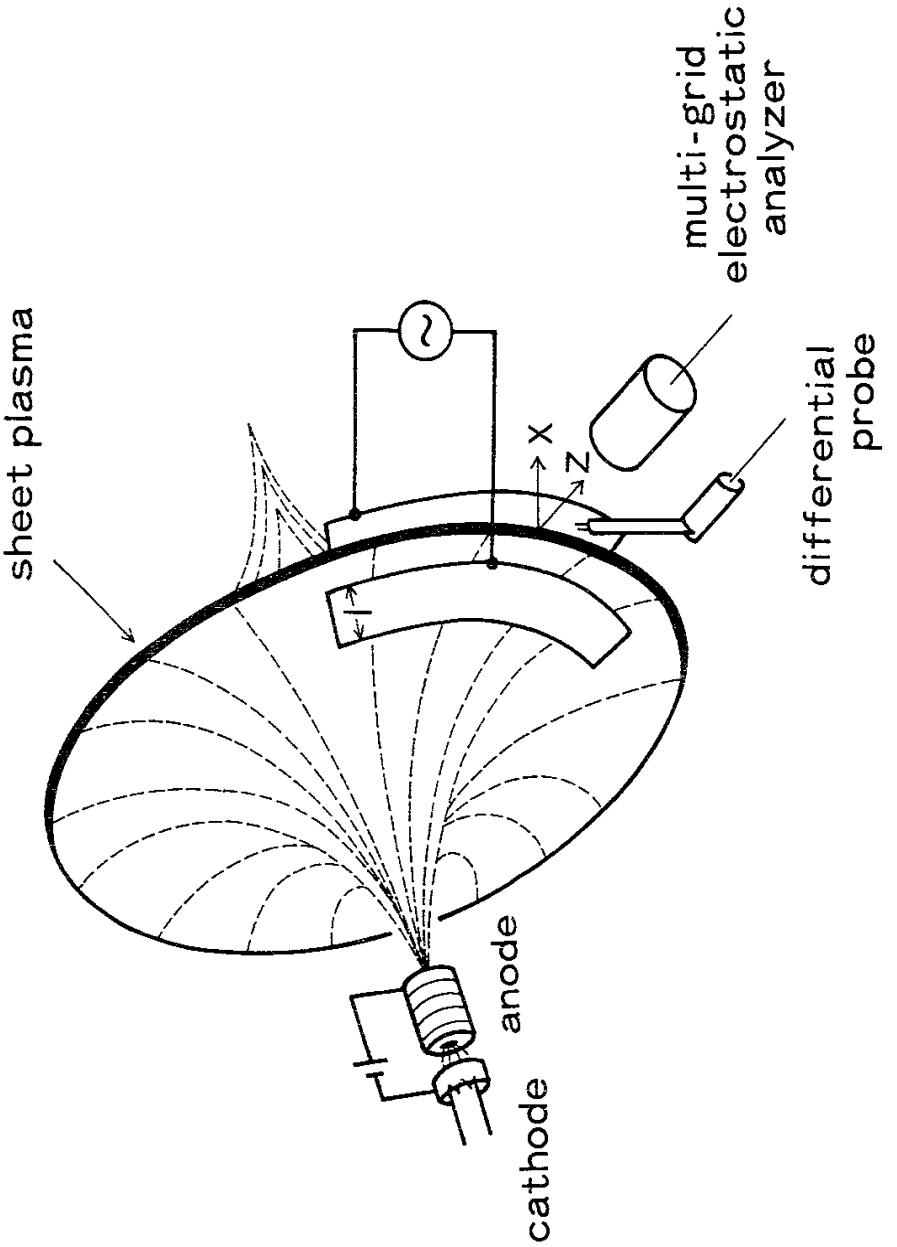
sheet plasma
multi-grid
electrostatic
analyzer
differential
probe
X
Z
anode
cathode

-Fig. 1-

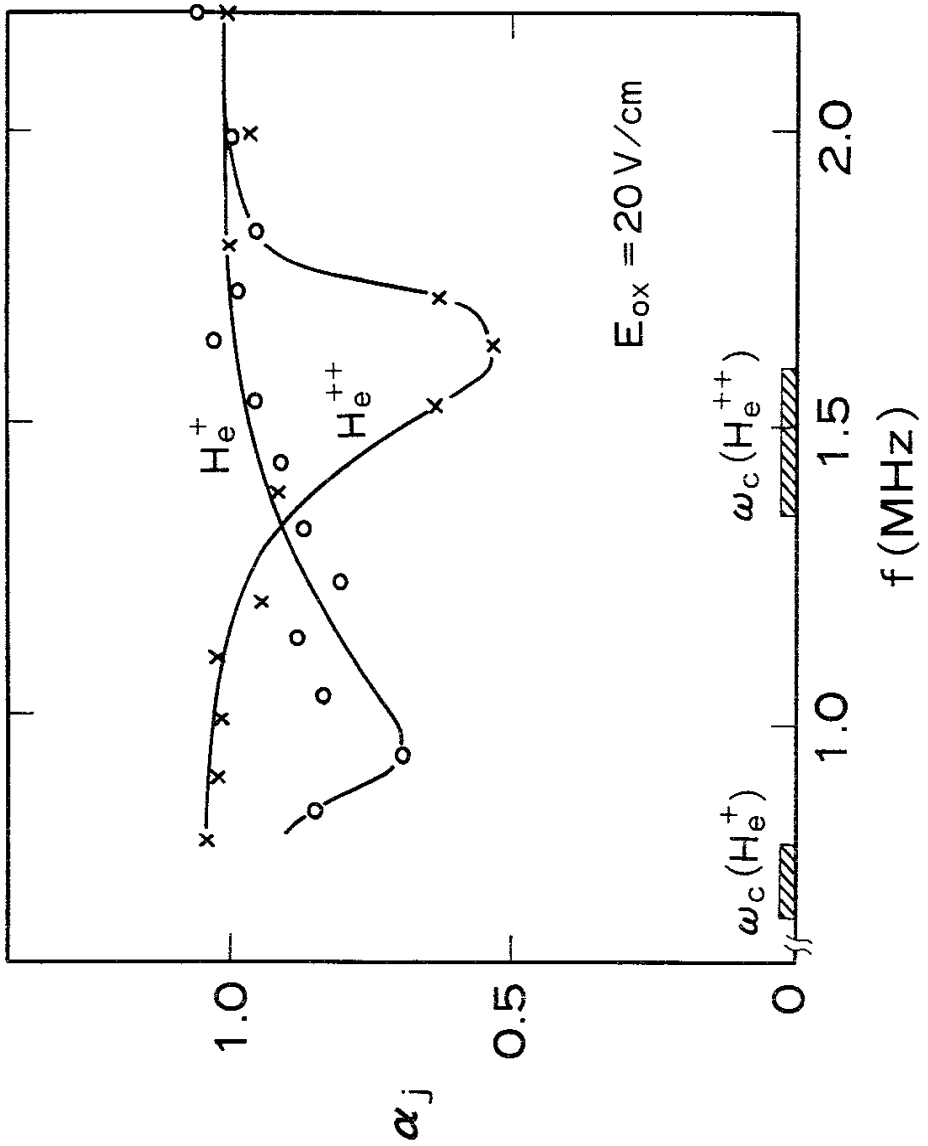

-Fig.2-

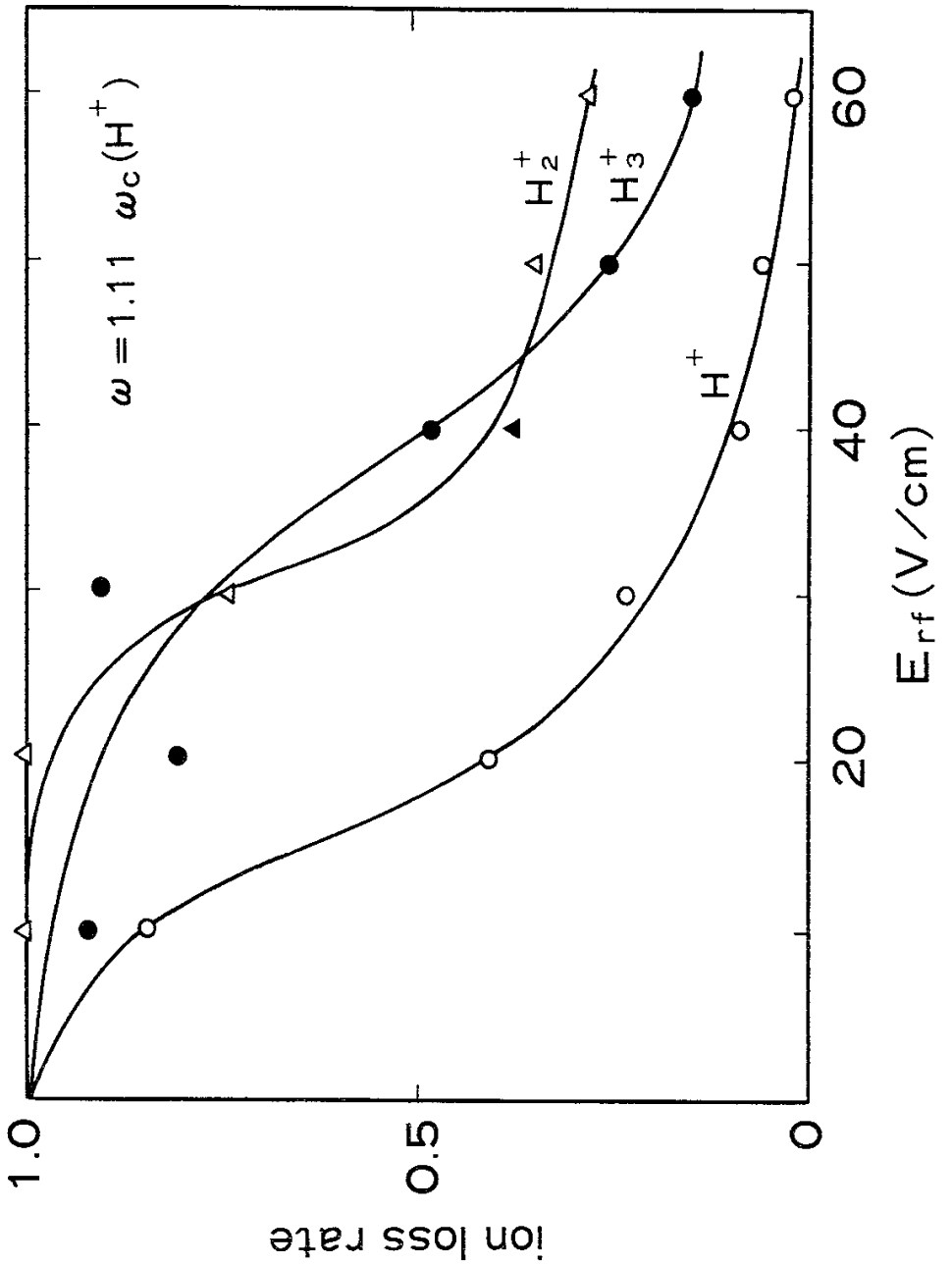

-Fig. 3-

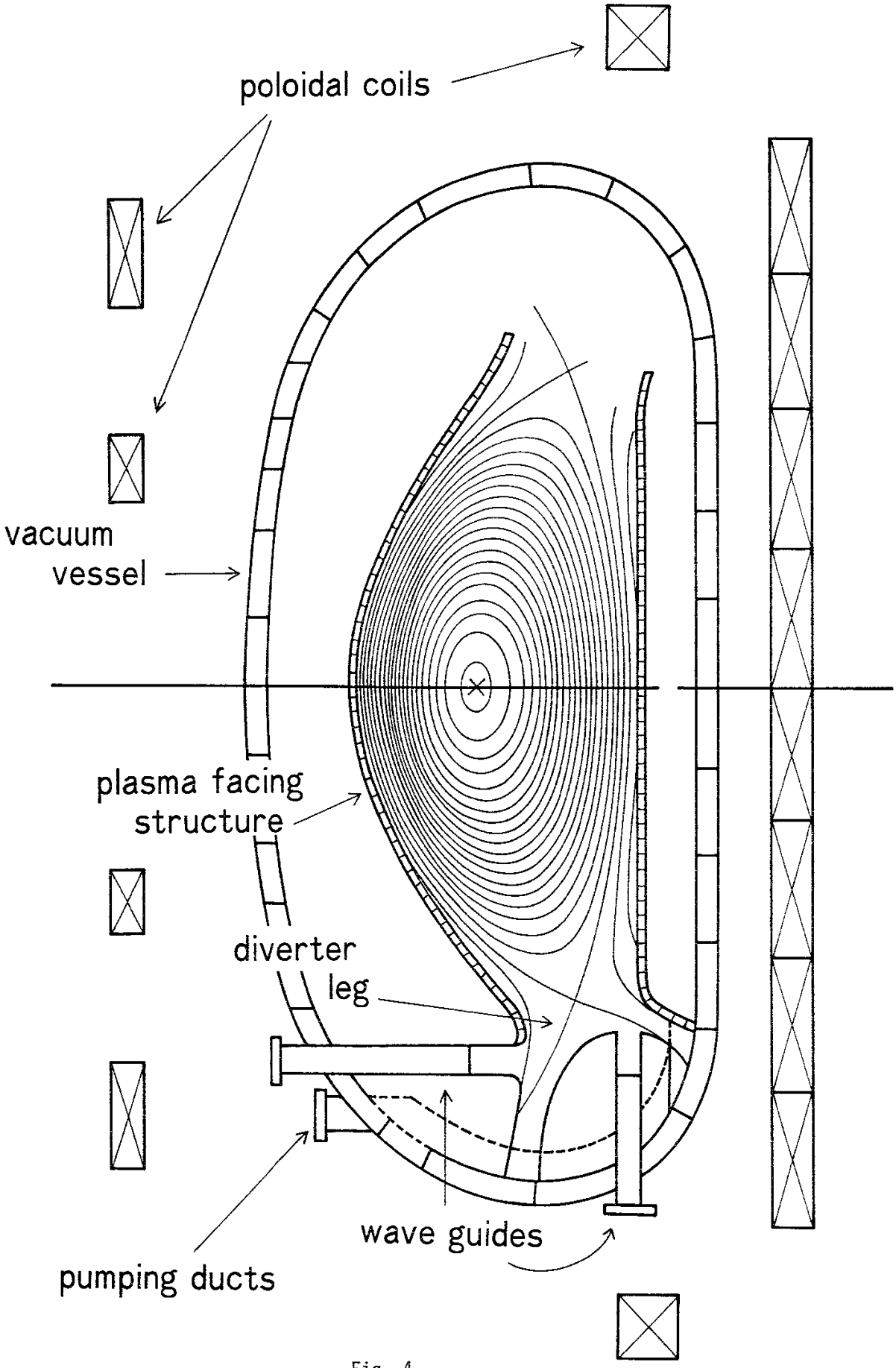
poloidal coils
vacuum
vessel
plasma facing
structure
diverter
leg
wave guides
pumping ducts

-Fig. 4-

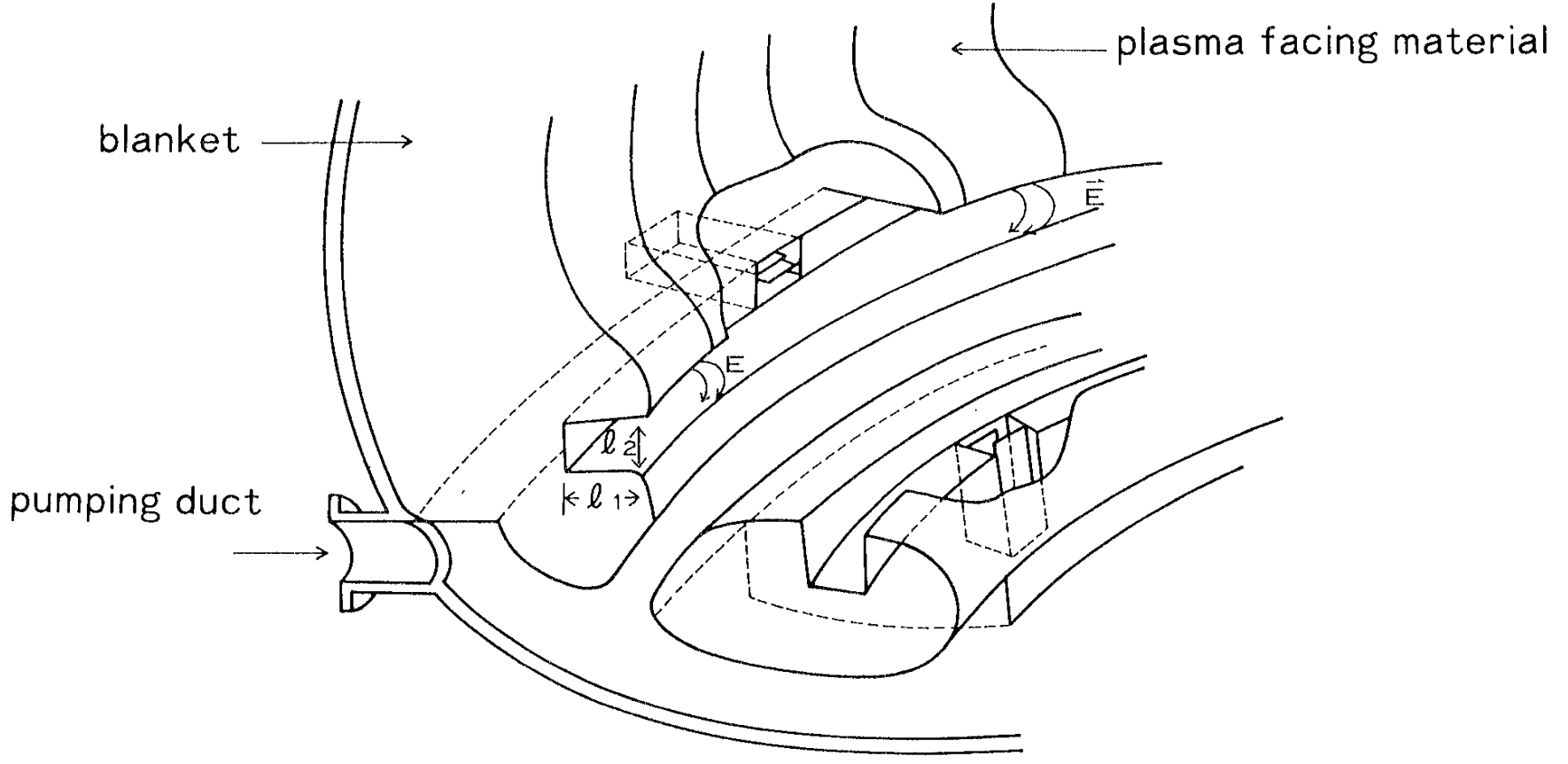

-Fig. 5-

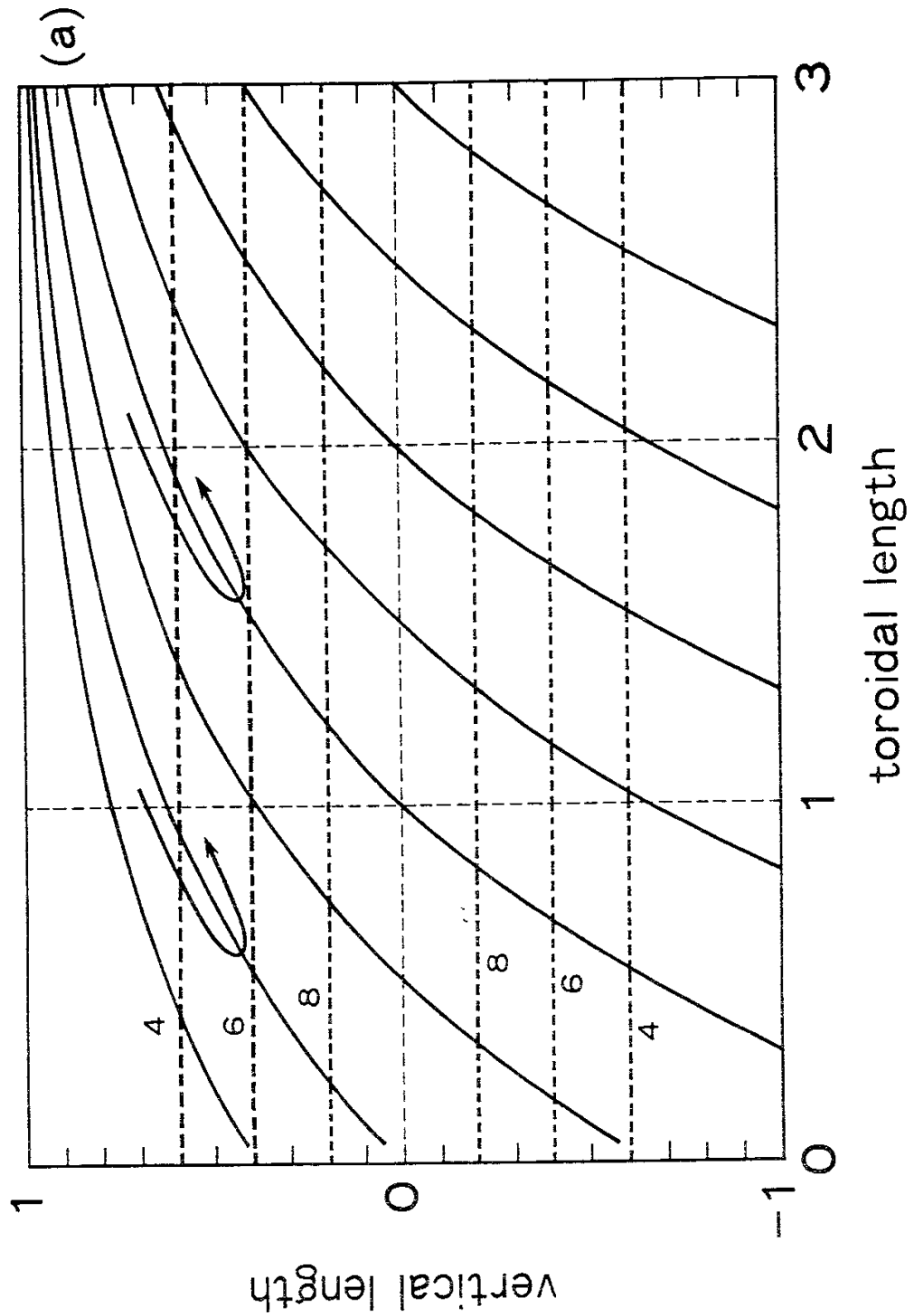

-Fig. 6 (a)-

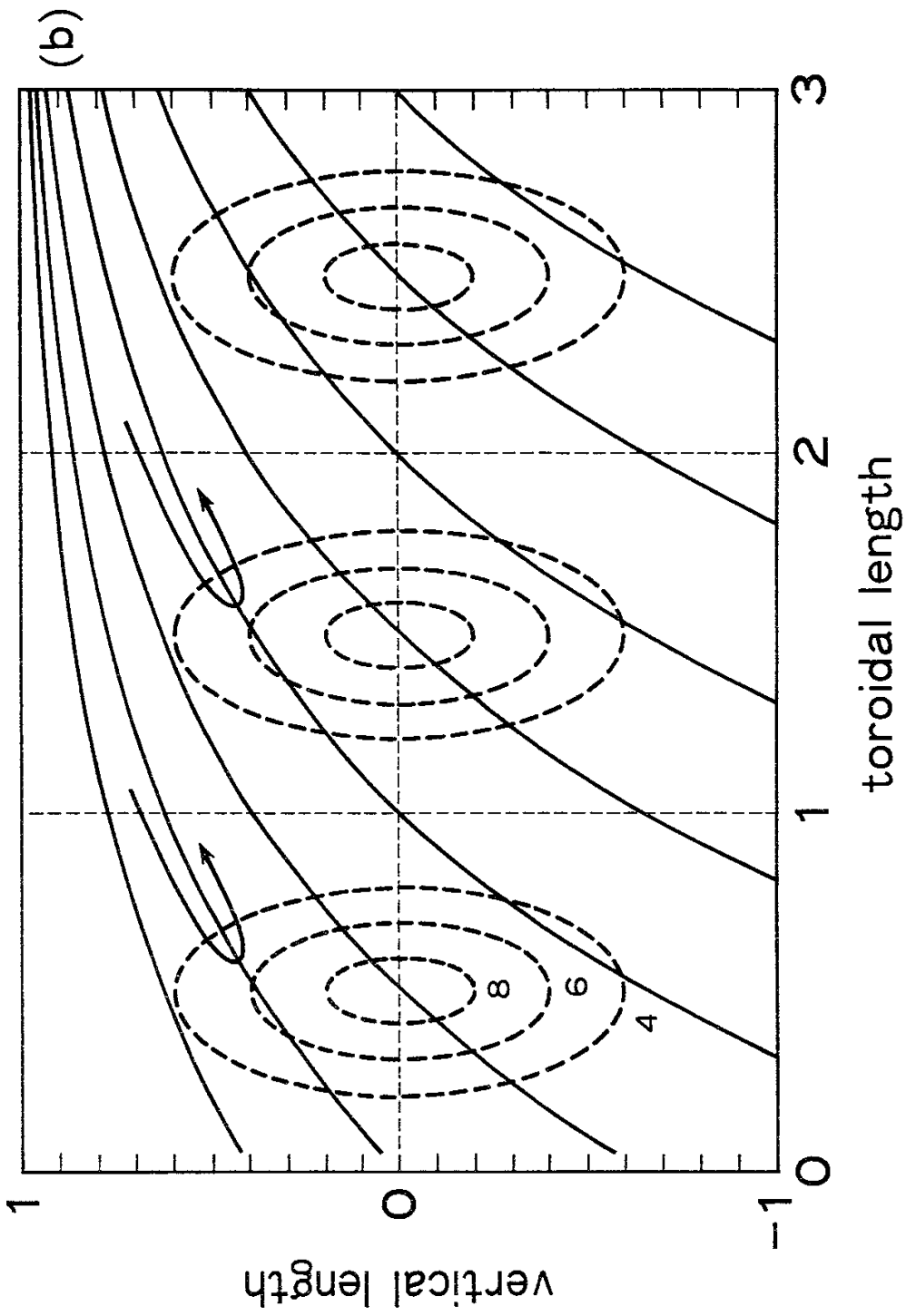

-Fig. 6 (b)-

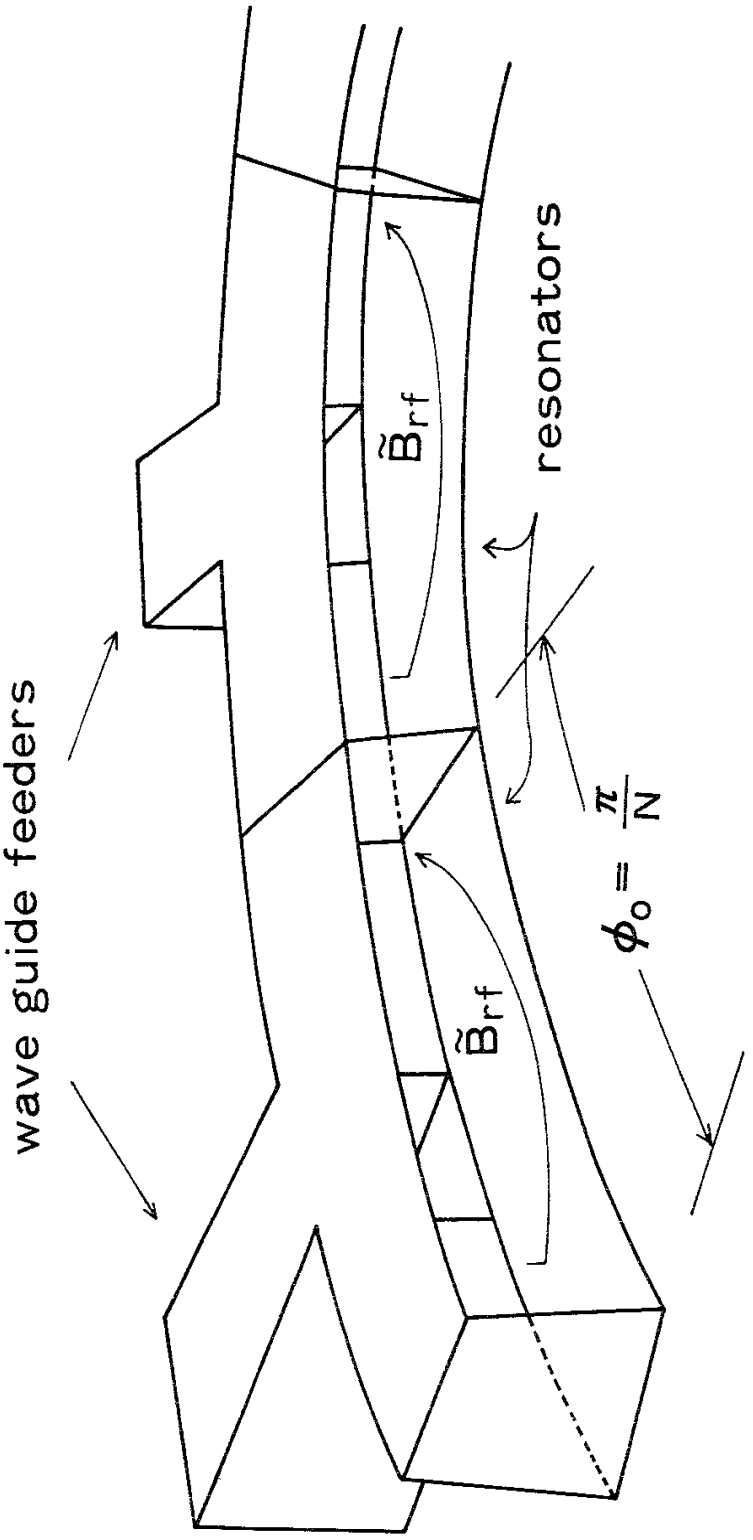
wave guide feeders
resonators
$\tilde{B}_{rf}$
$\tilde{B}_{rf}$
$\phi_o = \frac{\pi}{N}$

-Fig. 7-

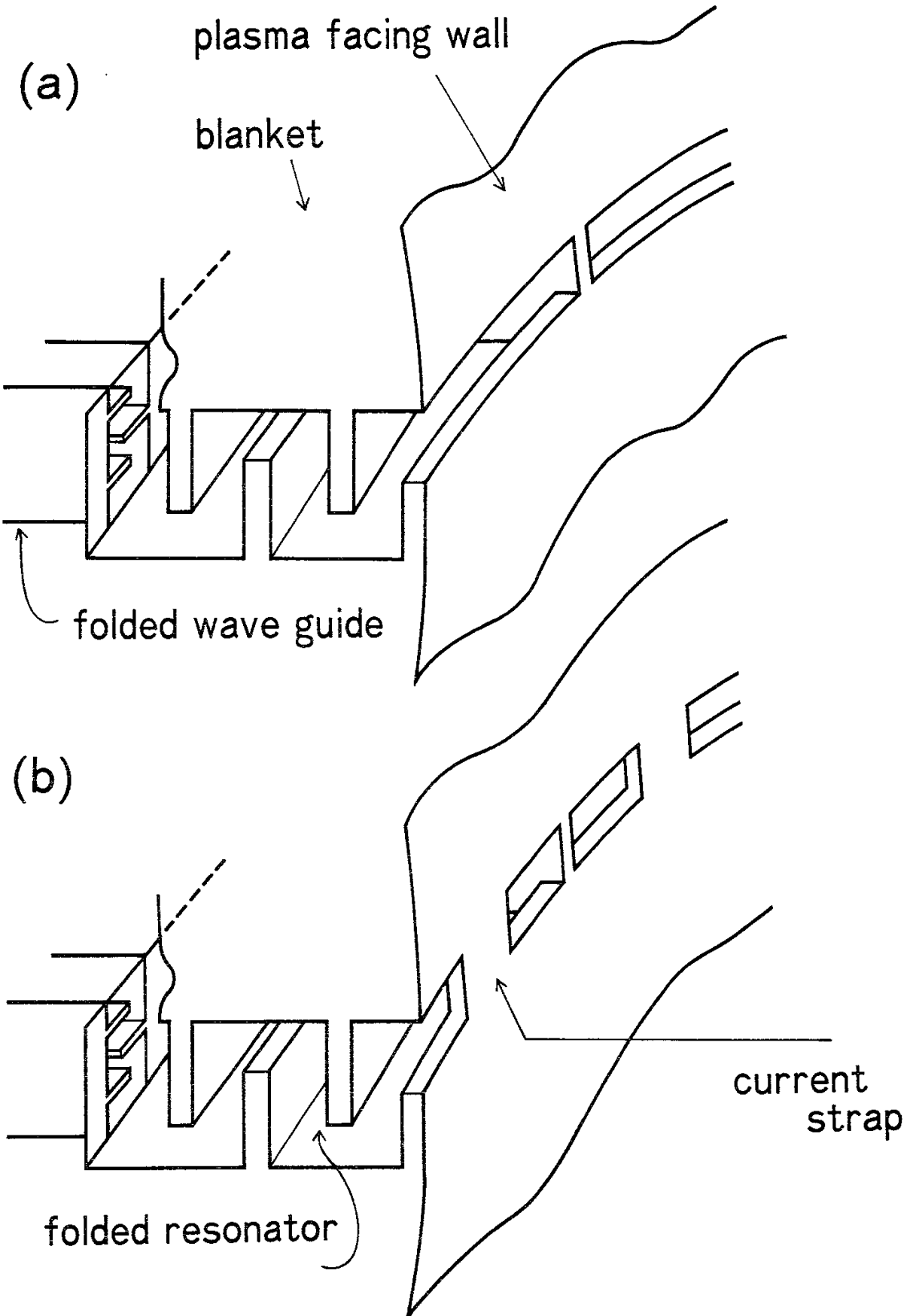
(a)
plasma facing wall
blanket
folded wave guide
(b)
current
strap
folded resonator

-Fig. 8-

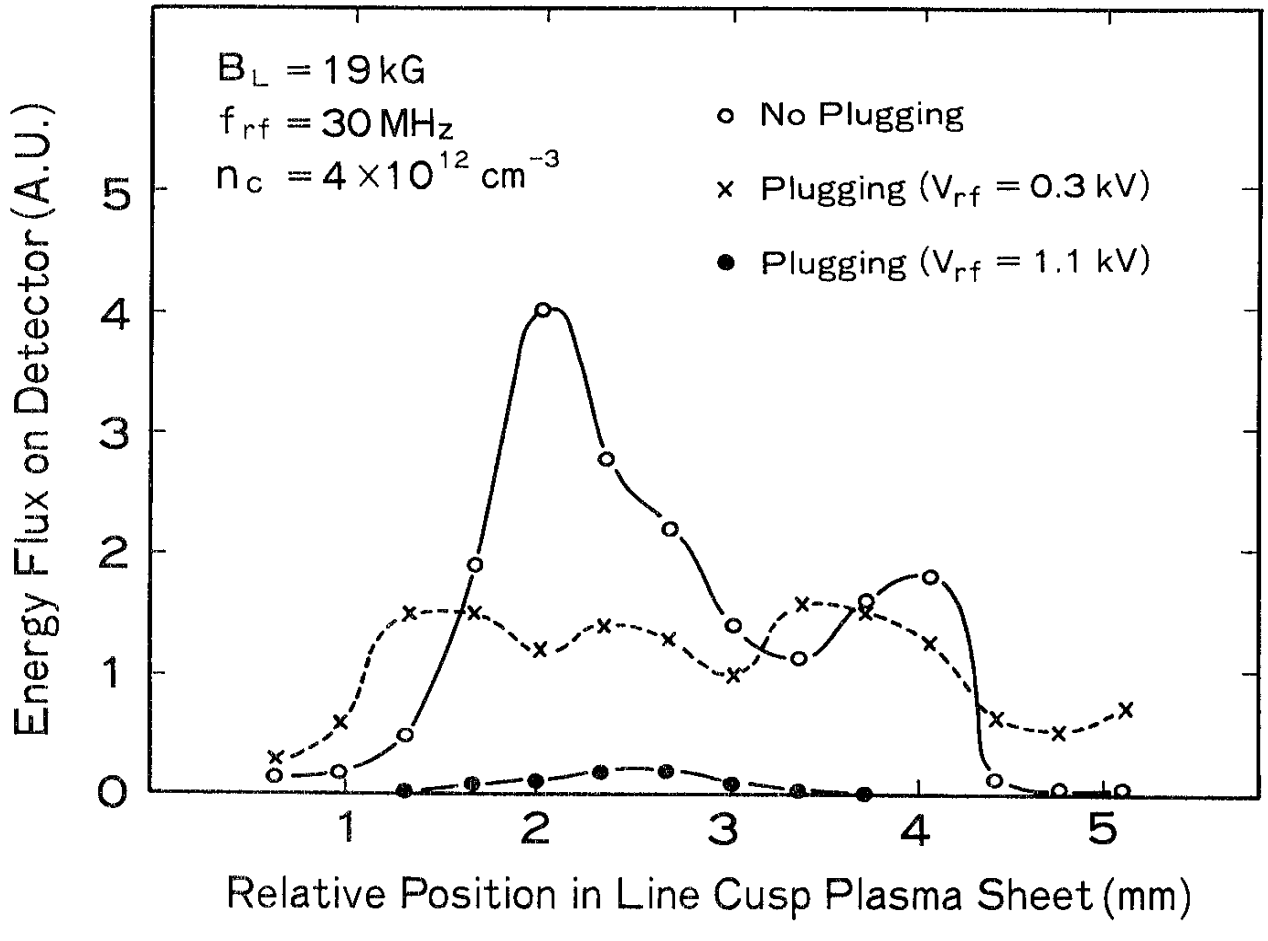
$B_L = 19\,kG$
$f_{rf} = 30\,MHz$
$n_c = 4 \times 10^{12}\,cm^{-3}$
o No Plugging
× Plugging ($V_{rf} = 0.3$ kV)
● Plugging ($V_{rf} = 1.1$ kV)
Energy Flux on Detector (A.U.)
0
1
2
3
4
5
1
2
3
4
5
Relative Position in Line Cusp Plasma Sheet (mm)

-Fig. 9-

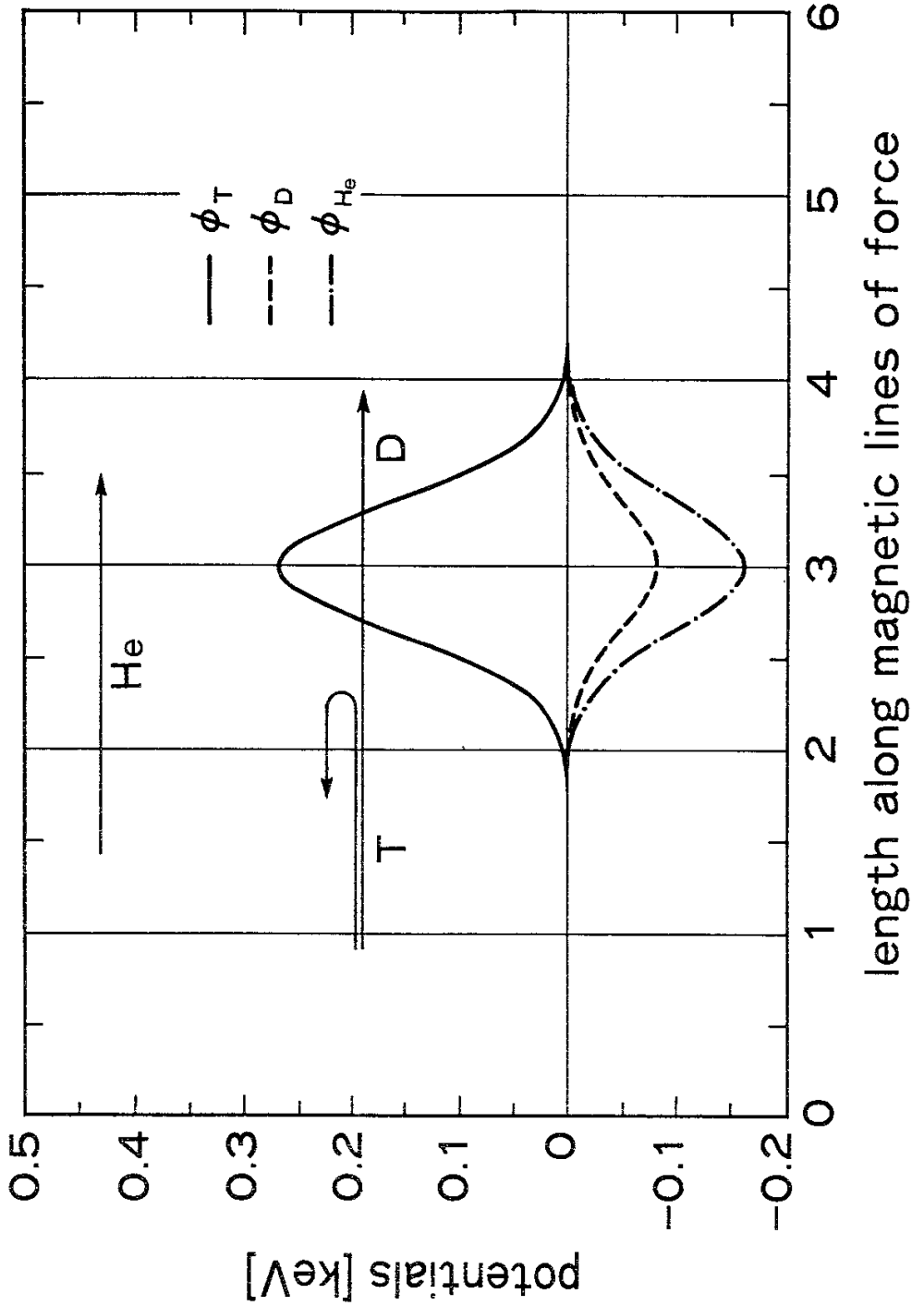
potentials [keV]
0.5
0.4
0.3
0.2
0.1
0
−0.1
−0.2
0
1
2
3
4
5
6
length along magnetic lines of force
ϕ_T
ϕ_D
ϕ_{He}
He
D
T

-Fig. 10-

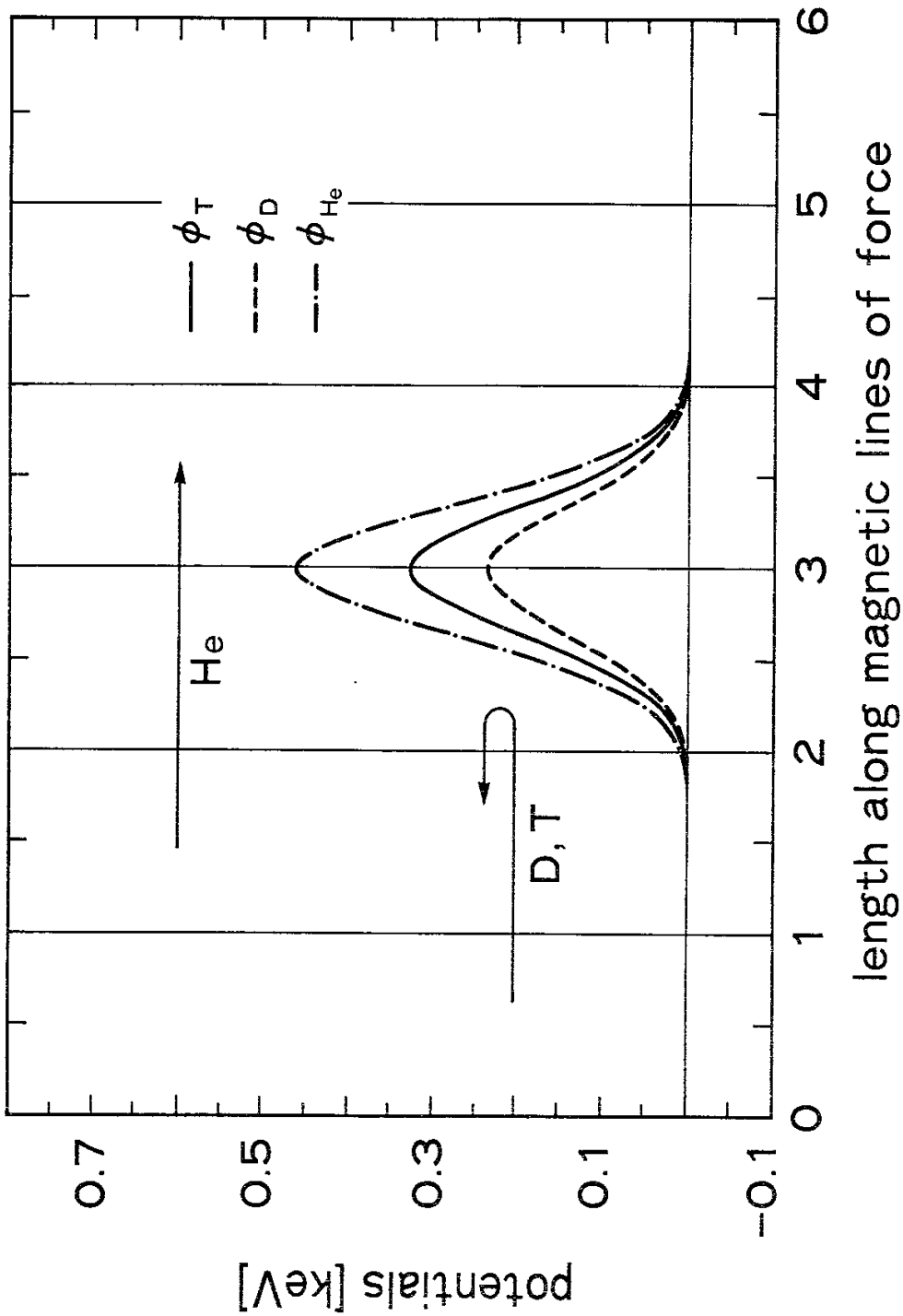
potentials [keV]
0.7
0.5
0.3
0.1
−0.1
0
1
2
3
4
5
6
length along magnetic lines of force
ϕ_T
ϕ_D
ϕ_{He}
He
D, T

-Fig. 11-

Recent Issues of NIFS Series

NIFS-177 N. Ohyabu, K. Yamazaki, I. Katanuma, H. Ji, T. Watanabe, K. Watanabe, H. Akao, K. Akaishi, T. Ono, H. Kaneko, T. Kawamura, Y. Kubota, N. Noda, A. Sagara, O. Motojima, M. Fujiwara and A. Iiyoshi, *Design Study of LHD Helical Divertor and High Temperature Divertor Plasma Operation* ; Sep. 1992

NIFS-178 H. Sanuki, K. Itoh and S.-I. Itoh, *Selfconsistent Analysis of Radial Electric Field and Fast Ion Losses in CHS Torsatron / Heliotron* ; Sep. 1992

NIFS-179 K. Toi, S. Morita, K. Kawahata, K. Ida, T. Watari, R. Kumazawa, A. Ando, Y. Oka, K. Ohkubo, Y. Hamada, K. Adati, R. Akiyama, S. Hidekuma, S. Hirokura, O. Kaneko, T. Kawamoto, Y. Kawasumi, M. Kojima, T. Kuroda, K. Masai, K. Narihara, Y. Ogawa, S. Okajima, M. Sakamoto, M. Sasao, K. Sato, K. N. Sato, T. Seki, F. Shimpo, S. Tanahashi, Y. Taniguchi, T. Tsuzuki, *New Features of L-H Transition in Limiter H-Modes of JIPP T-IIU* ; Sep. 1992

NIFS-180 H. Momota, Y. Tomita, A. Ishida, Y. Kohzaki, M. Ohnishi, S. Ohi, Y. Nakao and M. Nishikawa, *D-^{3}He Fueled FRC Reactor "Artemis-L"* ; Sep. 1992

NIFS-181 T. Watari, R. Kumazawa, T. Seki, Y. Yasaka, A. Ando, Y. Oka,O. Kaneko, K. Adati, R. Akiyama, Y. Hamada, S. Hidekuma, S. Hirokura, K. Ida, K. Kawahata, T. Kawamoto, Y. Kawasumi, S. Kitagawa, M. Kojima, T. Kuroda, K. Masai, S. Morita, K. Narihara, Y. Ogawa, K. Ohkubo, S. Okajima, T. Ozaki, M. Sakamoto, M. Sasao, K. Sato, K. N. Sato, F.Shimpo, H. Takahashi, S. Tanahasi, Y. Taniguchi, K. Toi, T. Tsuzuki and M. Ono, *The New Features of Ion Bernstein Wave Heating in JIPP T-IIU Tokamak* ;Sep, 1992

NIFS-182 K. Itoh, H. Sanuki and S.-I. Itoh, *Effect of Alpha Particles on Radial Electric Field Structure in Torsatron / Heliotron Reactor*; Sep. 1992

NIFS-183 S. Morimoto, M. Sato, H. Yamada, H. Ji, S. Okamura, S. Kubo, O. Motojima, M. Murakami, T. C. Jernigan, T. S. Bigelow, A. C. England, R. S. Isler, J. F. Lyon, C. H. Ma, D. A. Rasmussen, C. R. Schaich, J. B. Wilgen and J. L. Yarber, *Long Pulse Discharges Sustained by Second Harmonic Electron Cyclotron Heating Using a 35GH$_Z$ Gyrotron in the Advanced Toroidal Facility*; Sep. 1992

NIFS-184 S. Okamura, K. Hanatani, K. Nishimura, R. Akiyama, T. Amano, H. Arimoto, M. Fujiwara, M. Hosokawa, K. Ida, H. Idei, H. Iguchi, O. Kaneko, T. Kawamoto, S. Kubo, R. Kumazawa, K. Matsuoka, S. Morita, O. Motojima, T. Mutoh, N. Nakajima, N. Noda, M. Okamoto, T. Ozaki, A. Sagara, S. Sakakibara, H. Sanuki, T. Seki, T. Shoji,

F. Shimbo, C. Takahashi, Y. Takeiri, Y. Takita, K. Toi, K. Tsumori, M. Ueda, T. Watari, H. Yamada and I. Yamada, *Heating Experiments Using Neutral Beams with Variable Injection Angle and ICRF Waves in CHS* ; Sep. 1992

NIFS-185 H. Yamada, S. Morita, K. Ida, S. Okamura, H. Iguchi, S. Sakakibara, K. Nishimura, R. Akiyama, H. Arimoto, M. Fujiwara, K. Hanatani, S. P. Hirshman, K. Ichiguchi, H. Idei, O. Kaneko, T. Kawamoto, S. Kubo, D. K. Lee, K. Matsuoka, O, Motojima, T. Ozaki, V. D. Pustovitov, A. Sagara, H. Sanuki, T. Shoji, C. Takahashi, Y. Takeiri, Y. Takita, S. Tanahashi, J. Todoroki, K. Toi, K. Tsumori, M. Ueda and I. Yamada, *MHD and Confinement Characteristics in the High-β Regime on the CHS Low-Aspect-Ratio Heliotron / Torsatron* ; Sep. 1992

NIFS-186 S. Morita, H. Yamada, H. Iguchi, K. Adati, R. Akiyama, H. Arimoto, M. Fujiwara, Y. Hamada, K. Ida, H. Idei, O. Kaneko, K. Kawahata, T. Kawamoto, S. Kubo, R. Kumazawa, K. Matsuoka, T. Morisaki, K. Nishimura, S. Okamura, T. Ozaki, T. Seki, M. Sakurai, S, Sakakibara, A. Sagara, C. Takahashi, Y. Takeiri, H. Takenaga, Y. Takita, K. Toi, K. Tsumori, K. Uchino, M. Ueda, T. Watari, I. Yamada, *A Role of Neutral Hydrogen in CHS Plasmas with Reheat and Collapse and Comparison with JIPP T-IIU Tokamak Plasmas* ; Sep. 1992

NIFS-187 K. Ioth, S.-I. Itoh, A. Fukuyama, M. Yagi and M. Azumi, *Model of the L-Mode Confinement in Tokamaks* ; Sep. 1992

NIFS-188 K. Itoh, A. Fukuyama and S.-I. Itoh, *Beta-Limiting Phenomena in High-Aspect-Ratio Toroidal Helical Plasmas*; Oct. 1992

NIFS-189 K. Itoh, S. -I. Itoh and A. Fukuyama, *Cross Field Ion Motion at Sawtooth Crash* ; Oct. 1992

NIFS-190 N. Noda, Y. Kubota, A. Sagara, N. Ohyabu, K. Akaishi, H. Ji, O. Motojima, M. Hashiba, I. Fujita, T. Hino, T. Yamashina, T. Matsuda, T. Sogabe, T. Matsumoto, K. Kuroda, S. Yamazaki, H. Ise, J. Adachi and T. Suzuki, *Design Study on Divertor Plates of Large Helical Device (LHD)* ; Oct. 1992

NIFS-191 Y. Kondoh, Y. Hosaka and K. Ishii, *Kernel Optimum Nearly-Analytical Discretization (KOND) Algorithm Applied to Parabolic and Hyperbolic Equations* : Oct. 1992

NIFS-192 K. Itoh, M. Yagi, S.-I. Itoh, A. Fukuyama and M. Azumi, *L-Mode Confinement Model Based on Transport-MHD Theory in Tokamaks* ; Oct. 1992

NIFS-193 T. Watari, *Review of Japanese Results on Heating and Current*

Drive ; Oct. 1992

NIFS-194 Y. Kondoh, *Eigenfunction for Dissipative Dynamics Operator and Attractor of Dissipative Structure* ; Oct. 1992

NIFS-195 T. Watanabe, H. Oya, K. Watanabe and T. Sato, *Comprehensive Simulation Study on Local and Global Development of Auroral Arcs and Field-Aligned Potentials* ; Oct. 1992

NIFS-196 T. Mori, K. Akaishi, Y. Kubota, O. Motojima, M. Mushiaki, Y. Funato and Y. Hanaoka, *Pumping Experiment of Water on B and LaB_6 Films with Electron Beam Evaporator* ; Oct., 1992

NIFS-197 T. Kato and K. Masai, *X-ray Spectra from Hinotori Satellite and Suprathermal Electrons* ; Oct. 1992

NIFS-198 K. Toi, S. Okamura, H. Iguchi, H. Yamada, S. Morita, S. Sakakibara, K. Ida, K. Nishimura, K. Matsuoka, R. Akiyama, H. Arimoto, M. Fujiwara, M. Hosokawa, H. Idei, O. Kaneko, S. Kubo, A. Sagara, C. Takahashi, Y. Takeiri, Y. Takita, K. Tsumori, I. Yamada and H. Zushi, *Formation of H-mode Like Transport Barrier in the CHS Heliotron / Torsatron* ; Oct. 1992

NIFS-199 M. Tanaka, *A Kinetic Simulation of Low-Frequency Electromagnetic Phenomena in Inhomogeneous Plasmas of Three-Dimensions* ; Nov. 1992

NIFS-200 K. Itoh, S.-I. Itoh, H. Sanuki and A. Fukuyama, *Roles of Electric Field on Toroidal Magnetic Confinement*, Nov. 1992

NIFS-201 G. Gnudi and T. Hatori, *Hamiltonian for the Toroidal Helical Magnetic Field Lines in the Vacuum*; Nov. 1992

NIFS-202 K. Itoh, S.-I. Itoh and A. Fukuyama, *Physics of Transport Phenomena in Magnetic Confinement Plasmas*; Dec. 1992

NIFS-203 Y. Hamada, Y. Kawasumi, H. Iguchi, A. Fujisawa, Y. Abe and M. Takahashi, *Mesh Effect in a Parallel Plate Analyzer*; Dec. 1992

NIFS-204 T. Okada and H. Tazawa, *Two-Stream Instability for a Light Ion Beam -Plasma System with External Magnetic Field;* Dec. 1992

NIFS-205 M. Osakabe, S. Itoh, Y. Gotoh, M. Sasao and J. Fujita, *A Compact Neutron Counter Telescope with Thick Radiator (Cotetra) for Fusion Experiment*; Jan. 1993

NIFS-206 T. Yabe and F. Xiao, *Tracking Sharp Interface of Two Fluids by the CIP (Cubic-Interpolated Propagation) Scheme*, Jan. 1993

NIFS-207 A. Kageyama, K. Watanabe and T. Sato, *Simulation Study of MHD Dynamo : Convection in a Rotating Spherical Shell*; Feb. 1993

NIFS-208 M. Okamoto and S. Murakami, *Plasma Heating in Toroidal Systems*; Feb. 1993

NIFS-209 K. Masai, *Density Dependence of Line Intensities and Application to Plasma Diagnostics*; Feb. 1993

NIFS-210 K. Ohkubo, M. Hosokawa, S. Kubo, M. Sato, Y. Takita and T. Kuroda, *R&D of Transmission Lines for ECH System* ; Feb. 1993

NIFS-211 A. A. Shishkin, K. Y. Watanabe, K. Yamazaki, O. Motojima, D. L. Grekov, M. S. Smirnova and A. V. Zolotukhin, *Some Features of Particle Orbit Behavior in LHD Configurations*; Mar. 1993

NIFS-212 Y. Kondoh, Y. Hosaka and J.-L. Liang, *Demonstration for Novel Self-organization Theory by Three-Dimensional Magnetohydrodynamic Simulation*; Mar. 1993

NIFS-213 K. Itoh, H. Sanuki and S.-I. Itoh, *Thermal and Electric Oscillation Driven by Orbit Loss in Helical Systems*; Mar. 1993

NIFS-214 T. Yamagishi, *Effect of Continuous Eigenvalue Spectrum on Plasma Transport in Toroidal Systems*; Mar. 1993

NIFS-215 K. Ida, K. Itoh, S.-I.Itoh, Y. Miura, JFT-2M Group and A. Fukuyama, *Thickness of the Layer of Strong Radial Electric Field in JFT-2M H-mode Plasmas*; Apr. 1993

NIFS-216 M. Yagi, K. Itoh, S.-I. Itoh, A. Fukuyama and M. Azumi, *Analysis of Current Diffusive Ballooning Mode*; Apr. 1993

NIFS-217 J. Guasp, K. Yamazaki and O. Motojima, *Particle Orbit Analysis for LHD Helical Axis Configurations* ; Apr. 1993

NIFS-218 T. Yabe, T. Ito and M. Okazaki, *Holography Machine HORN-1 for Computer-aided Retrieve of Virtual Three-dimensional Image* ; Apr. 1993

NIFS-219 K. Itoh, S.-I. Itoh, A. Fukuyama, M. Yagi and M. Azumi, *Self-sustained Turbulence and L-Mode Confinement in Toroidal Plasmas* ; Apr. 1993